PROTONATION EFFECTS ON DYNAMIC FLUX PROPERTIES OF AQUEOUS METAL COMPLEXES

Herman P. van LEEUWEN[a,*] and Raewyn M. TOWN[b]

[a] *Laboratory of Physical Chemistry and Colloid Science, Wageningen University, Dreijenplein 6, 6703 HB Wageningen, The Netherlands; e-mail: herman.vanleeuwen@wur.nl*

[b] *Institute for Physics and Chemistry, University of Southern Denmark, Campusvej 55, 5230 Odense, Denmark; e-mail: rmt@ifk.sdu.dk*

Received July 29, 2009
Accepted September 21, 2009
Published online December 9, 2009

This article has been written with the intention to commemorate and honour the pioneering research on kinetic Faradaic currents performed by Professor Jaroslav Heyrovský and his collaborators Rudolf Brdička, Jaroslav Koutecký and Jiří Koryta.

The degree of (de)protonation of aqueous metal species has significant consequences for the kinetics of complex formation/dissociation. All protonated forms of both the ligand and the hydrated central metal ion contribute to the rate of complex formation to an extent weighted by the pertaining outer-sphere stabilities. Likewise, the lifetime of the uncomplexed metal is determined by all the various protonated ligand species. Therefore, the interfacial reaction layer thickness, μ, and the ensuing kinetic flux, J_{kin}, are more involved than in the conventional case. All inner-sphere complexes contribute to the overall rate of dissociation, as weighted by their respective rate constants for dissociation, k_d. The presence of inner-sphere deprotonated H_2O, or of outer-sphere protonated ligand, generally has a great impact on k_d of the inner-sphere complex. Consequently, the overall flux can be dominated by a species that is a minor component of the bulk speciation. The concepts are shown to provide a good description of experimental stripping chronopotentiometric data for several protonated metal–ligand systems.

Keywords: Eigen mechanism; Dynamic metal speciation; Association rate; Dissociation rate.

A rigorous framework for analysis of metal speciation dynamics is fundamental for understanding and prediction of a range of environmental and biological processes. This includes sink/source functioning of ecosystems, bioaccumulation of chemicals, toxicity of chemical species, as well as interpretation of signals from dynamic speciation techniques[1]. For the case of voltammetry, the overall flux of species to the electrode surface results from the coupled diffusion and kinetics of interconversion of various metal spe-

doi:10.1135/cccc2009091

cies. In this context, protonation of metal species is an important factor to be considered. It is long established that the degree of ligand protonation influences metal complexation equilibria: conditional stability constants are often invoked to describe the effective binding strength at a given pH. Protonation is also of great importance in the kinetics of metal complexation. It is, for example, responsible for enhanced rates in what has been called 'acid-catalyzed' or 'proton-assisted' dissociation[2–4]. At the other end of the pH scale, 'base-catalyzed' dissociation is reported for metal complexes containing inner-sphere hydroxide as a 'co-ligand' [4]. Here we are reviewing recent progress in the development of a generic framework to quantitatively describe the impact of protonation on metal speciation dynamics. The interpretation is based on the Eigen mechanism principles considering the influence of the (de)protonation degree of both the ligand *and* the hydrated metal ion in the complex formation *and* dissociation processes. The consequences for interfacial reaction layers and ensuing kinetic fluxes, introduced in the 1950s by the Heyrovský school[5–7] and so well laid out in Chapter XVII of the Heyrovský–Kůta book[7], are considered in detail. The concepts are illustrated by stripping chronopotentiometric (SCP) data for a variety of systems involving a range of protonated outer-sphere and inner-sphere complexes.

THEORETICAL

In a complex system, the degree of protonation of the ligand and complex species influences the rates of both complex formation and dissociation. A comprehensive analysis calls for consideration of all species involved in the kinetically relevant precursor outer-sphere complexes and the eventual inner-sphere complexes, even if they are minor species in terms of bulk equilibrium speciation. Our focus here is on relatively small, well-defined multidentate ligands; additional features are known to be involved in the kinetics of metal complexation with colloidal and polyelectrolytic ligands[8].

Rates of Complex Formation/Dissociation

Many complex formation reactions in aqueous solution follow the Eigen mechanism, i.e. formation of an outer-sphere complex between the hydrated metal ion M, and the ligand L, followed by a generally slower rate-limiting dehydration step[9]. The rate of complex formation, k_a, is thus determined by (i) the stability constant for the intermediate outer-sphere complex, K^{os}, and (ii) the rate constant for water substitution in the inner

coordination sphere of the metal ion, k_w. Compilations of experimentally determined k_w values are available, and results typically span up to an order of magnitude for a given metal ion[10]. The overall scheme for the formation of 1:1 inner-sphere metal–ligand complexes, which includes all the various degrees of protonation of the metal and ligand species can be written as

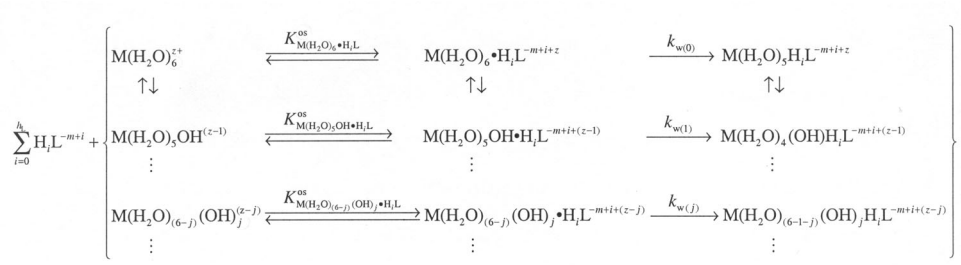

(*1*)

where • denotes outer-sphere association; index *i* denotes the number of protons attached to the fully deprotonated L^{-m} running from 0 to h_L; index *j* is the number of protons removed from the inner-shell H_2O in $M(H_2O)_6^{z+}$ running from 0 to h_M. Note that (i) h_L is not necessarily identical to *m*, e.g. for EDTA, $h_L = 6$ and $m = 4$, and (ii) for most practical purposes h_M does not exceed 4 or 5.

Protonation reactions are very fast[11], so the various protonated/deprotonated forms can be considered to be in equilibrium: their equilibrium concentrations are relevant for complex formation/dissociation kinetics. Equation (*1*) expresses that *all* protonated forms of L and M contribute to k_a to an extent weighted by their respective outer-sphere ion pair stabilities[12]. Thus the overall rate of complex formation, R_a, sums the contributions from all outer-sphere complexes, i.e.

$$R_a = \sum_{i=0}^{h_L} \sum_{j=0}^{h_M} [k_{w(j)} K^{os}_{M(OH)_j \bullet H_i L} c_{M(OH)_j} c_{H_i L}]. \qquad (2)$$

The dehydration rate constant, k_w, is not significantly affected by the presence or absence of a proton in the complexing ligand, but it is strongly impacted by the degree of deprotonation of water in the inner hydration sphere of the coordinating metal species. Whilst k_w values have been reported for Fe(III) with various degrees of hydroxylation[10–17], there is a paucity of such data for other metal ions. Divalent ions show k_w values greater than trivalent ones; for Mn, Fe, and Co, the k_w values for the divalent ion

$M(H_2O)_6^{2+}$ are approximately 30 times higher[18] than those for the monohydroxy form of the corresponding trivalent ion $M(H_2O)_5OH^{2+}$.

Following Fuoss, the magnitude of K^{os} is estimated on the basis of Boltzmann statistics for the metal ion in the free state and the ion-pair state[19]

$$K^{os} = \frac{4\pi}{3} N_A a_g^3 \exp(-\boldsymbol{U}^{os}) \qquad (3)$$

where a_g is the geometrical center-to-center distance between M and L, and $\boldsymbol{U}^{os} = U^{os}/kT$. For a composite ligand incorporating different charged sites, the interionic potential $\boldsymbol{U}^{os}$ sums all electrostatic interactions between the central metal ion and the various charges i on L, with inclusion of screening by the surrounding electrolyte solution[20]

$$\boldsymbol{U}^{os} = \frac{z_M e^2}{4\pi\varepsilon_0\varepsilon} \sum_i \frac{z_i}{a_i} \left[1 - \frac{\kappa a_i}{1 + \kappa a_i} \right] \qquad (4)$$

where z_i is the charge number of site i, $\varepsilon_0\varepsilon$ is the dielectric permittivity of the electrolyte solution, a_i is the center-to-center distance between i and M, and κ is the reciprocal Debye length of the electrolyte solution. As detailed previously[12], the *change* in intramolecular electrostatic interactions between different charged sites of a given L upon formation of the ion pair are counted in $\boldsymbol{U}^{os}$. Within the broad framework of chemodynamics of metals in environmental systems, the computation of $\boldsymbol{U}^{os}$ for colloidal ligands with various charge distributions has recently been reviewed in detail[8].

In general, the distribution of ligand species is shifted to increasingly lower degrees of protonation on going from the noncoordinated ligand in the bulk solution to outer-sphere complexes and the ensuing inner-sphere complexes (e.g. Cd(II)–EDTA). Conversely, for inner-sphere complexes involving inner-sphere OH^-, the effective degree of deprotonation of the metal ion decreases when going from bulk solution to inner-sphere complex, as the incoming ligand displaces the deprotonated water in the inner hydration sphere of the metal ion.

The degree of (de)protonation of an inner-sphere complex can have a drastic impact on its rate of dissociation. Here we focus on the kinetic implications of (i) H^+ occupying a potential coordinating site in the ligand, and (ii) water molecules in the inner hydration sphere of the metal ion being deprotonated to some extent. As compared to ML, both the ligand-protonated MH_iL, and metal-deprotonated $M(OH)_jL$, inner-sphere com-

plexes are generally significantly weaker and have higher rates of dissociation. In this context, kinetic studies can aid in sorting out proton linkage isomerism, i.e. whether a complex formulated as $MH_{-1}L$ corresponds to a deprotonated water molecule in the inner hydration sphere of M or to a deprotonated remote site on L [21,22].

Complex Formation/Dissociation in Interfacial Reactions

For the case of an interfacial process that involves consumption of M, e.g. reduction at a voltammetric electrode, interpretation of the interfacial flux requires knowledge of the reaction layer. In a conventional reaction layer for a simple M + ML system, the thickness μ is determined by the mean diffusional displacement of free M during its lifetime, τ_M

$$\mu = (D_M \tau_M)^{1/2} . \qquad (5)$$

For a sufficiently stable complex ML and negligible depletion, the ensuing kinetic flux, J_{kin}, is

$$J_{kin} = k_d c^0_{ML} \mu \qquad (6)$$

where superscript 0 denotes the concentration at the interface. The reaction layer is the layer of solution adjacent to the electrode surface, within which the equilibrium between the complex species and M cannot be maintained. This feature is the basis for Koutecký–Koryta's ingenious two-state approximation[7,23] (the KK approximation) in which the diffusion layer is spatially divided into a non-labile and a labile region separated by the boundary of the reaction layer. Within the reaction layer, the contribution from the complex to the flux is considered to be purely kinetic (Eq. (*6*)), whereas beyond the reaction layer, the kinetics are assumed to be infinitely fast so that the profiles of the complex and M obey the equilibrium condition (Fig. 1). The KK approximation has been rigorously evaluated and was found to have far-reaching validity in the whole kinetic range from nonlabile to labile complexes for any metal-to-ligand ratio[24].

Recently, these fundamental concepts have been extended to describe fluxes in systems containing various protonated species[12,25,26]. The flux, J_{kin}, from the dissociation of all relevant inner-sphere complexes is

$$J_{kin} = \left\{ \sum_{i=0}^{h_L} \sum_{j=0}^{h_M} k_{dM(OH)_j H_i L} c^0_{M(OH)_j H_i L} \right\} \mu_{eff} . \qquad (7)$$

Just like Eq. (*6*), Eq. (*7*) holds for fluxes that are kinetically controlled, i.e. implying that they are not limited by diffusion[27]. The effective reaction layer thickness, μ_{eff}, is defined by τ_M (Eq. (*5*)) with the re-association rate contributions from all the differently protonated species, i.e.

$$\frac{1}{\tau_M} = \frac{R_a}{c_M} = \sum_{i=0}^{h_L} \sum_{j=0}^{h_M} k_{wM(H_2O)_{6-j}(OH)_j} K^{os}_{M(H_2O)_{6-j}(OH)_j \cdot H_iL} (c_{M(OH)_j} / c_M) c_{H_iL} \qquad (8)$$

where c_M includes all the $M(OH)_j$ species, for any j, since these are in fast protolytic equilibrium with each other.

In this context we mention that a more elaborate expression for the reaction layer thickness has been developed to describe fluxes in *mixtures of different*+ *ligands*, forming complexes of any strength and mobility that impact on the overall reassociation rate of metal and ligand[28,29]. This situation is shown schematically in Fig. 1. However, it should be noted that the extent of validity of the KK approximation is not the same for species with differ-

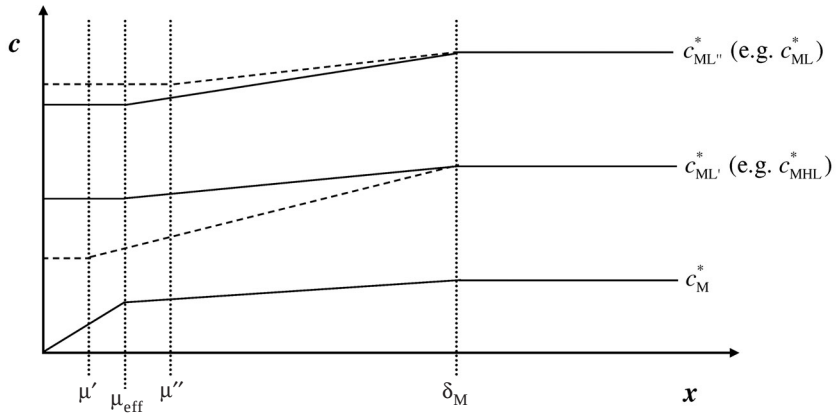

FIG. 1

Schematic concentration profiles for metal species in a system containing a single ligand, L′ or L″ (dashed curves), as compared with a mixture of the two (solid curves). As drawn, the lability of the complex with ligand L′ is greater than that with ligand L″. Reaction layer thicknesses for the two individual cases and for the mixture are indicated as μ′, μ″, and μ_{eff}, respectively; δ_M is the diffusion layer thickness for free M

+ Ligands of different chemical nature, not just differing in protonation.

ent labilities and, hence, that the nature of the averaging is rather involved. Detailed numerical analysis is required to establish the most rigorous approach for analysis of these systems.

Degree of Lability

The concept of lability describes the ability of complexes to maintain equilibrium with the free metal ion[++], M, under conditions of an ongoing interfacial process involving conversion of M, e.g. reduction at a voltammetric electrode[30]. For the simplest case, the schematic representation is

$$\begin{array}{ccccc} \mathrm{M} & + & \mathrm{L} & \underset{k_\mathrm{d}}{\overset{k_\mathrm{a}}{\rightleftharpoons}} & \mathrm{ML} \\ \downarrow & & & & \\ \mathrm{M}^0 & & & & \end{array} \qquad (9)$$

The degree of lability, ξ, quantitatively expresses the contribution of the dissociating complex ML to the eventual metal flux, *J*, normalized with respect to its maximum, purely diffusion-controlled, contribution, J_{dif} [31]. As an example of the flux of various inner-sphere complex species with different degrees of protonation, $\mathrm{MH}_i\mathrm{L}$, ML, $\mathrm{M(OH)}_j\mathrm{L}$, and different k_d, towards a spherical microelectrode with radius r_0, the overall ξ is given by

$$\xi = \frac{J - J_{\mathrm{free}}}{J_{\mathrm{dif}} - J_{\mathrm{free}}} = \frac{J - D_\mathrm{M} c_{\mathrm{M,free}} / r_0}{\sum_{i=0}^{h_\mathrm{L}} \sum_{j=0}^{h_\mathrm{M}} D_{\mathrm{M(OH)}_j \mathrm{H}_i\mathrm{L}} c_{\mathrm{M(OH)}_j \mathrm{H}_i\mathrm{L}} / r_0 - D_\mathrm{M} c_{\mathrm{M,free}} / r_0} \qquad (10)$$

where the free metal flux, J_{free}, includes $\mathrm{M(OH)}_j$ species when present, and *J* is the actual flux. For *J* well below J_{dif}, the term $J - J_{\mathrm{free}}$ is of kinetic nature and Eq. (*7*) applies. An appropriate expression for ξ can also be written for higher-order complexes.

Stripping Chronopotentiometry at Scanned Deposition Potential (SSCP)

Various modes of voltammetry, including stripping voltammetry (SV), are sensitive to kinetic effects. In recent years, stripping chronopotentiometry

++In the present context, the distribution of "free" metal over $\mathrm{M(H_2O)_6^{z+}}$ and $\mathrm{M(H_2O)_{6-}}_j\mathrm{(OH)}_j^{(z-j)+}$ is immaterial since equilibrium is sustained by a fast proton exchange.

(SCP) in its scanned deposition potential mode (SSCP) has emerged as a powerful tool for characterisation of dynamic metal speciation[32]. The deposition step in SCP is the same as that in SV (reduction of the target metal ion at a fixed potential for a specified time), but the accumulated metal is quantified by application of a constant oxidizing current, I_s. The analytical SCP signal is thus the time for reoxidation, τ. The depletive SCP mode (low I_s) gives a correct measure of the accumulated metal, even in the presence of induced metal adsorption[33]. SSCP waves (plots of τ as a function of deposition potential, E_d) can be used to determine metal complexation parameters in a manner equivalent to the conventional DeFord–Hume analysis of position and height of voltammetric waves[34–36]. Application of the KK approximation enables formulation of an expression of the SSCP wave for a complex system with limited rates of formation/dissociation[37]. The theory provides a quantitative description of SSCP waves measured for Cd(II)–nitrilotriacetic acid (NTA) at conventional electrodes and microelectrodes, at various degrees of lability. Dynamic speciation characteristics have been unambiguously identified and distinguished from those due to irreversibility in the electrochemical reaction or heterogeneity in the chemical speciation.

The SCP technique used in this work is of a steady-state nature, as is stripping voltammetry. The interfacial flux is immediately proportional to the current. These techniques can be applied to determination of kinetic properties over a certain range by either changing the diffusion layer thickness at a conventional electrode, or by use of microelectrodes of various radii. Development of microelectrode arrays, with a range of electrode sizes on the same chip, facilitates future voltammetric measurements over a dynamic range.

RESULTS AND DISCUSSION

To illustrate the theoretical concepts presented above we have measured the influence of protonation on the stripping lability of several metal complex systems at conventional electrodes and microelectrodes. The systems studied cover (i) 1:1 ML complexes, (ii) MHL complexes, and (iii) higher-order ML_2 complexes as well as features in $M(OH)_jL$ systems.

1:1 ML Inner-Sphere Complexes

For the case of a 1:1 ML complex, all of the various protonated forms of L contribute to the overall k_a (Eq. (*2*)). Here we consider the situation where

ML is the only eventual inner-sphere complex formed. Cd(II) complexes with 1,2-diaminoethane-*N*,*N*′-diacetic acid (EDDA) fall into this category, and the measured microelectrodic J_{kin} is well described by the theoretical framework. Figure 2 illustrates that the experimental data follow the trend prescribed by the combined impact of both the unprotonated and protonated outer-sphere complexes (solid curves). Consideration of only unprotonated outer-sphere complexes (long-dashed curves), or only protonated outer-sphere complexes (short-dashed curves) in the rate-determining step increasingly overestimates the lifetime of free M and μ as pH decreases or increases, respectively.

MHL and ML Inner-Sphere Complexes

Ethylenediaminetetraacetic acid, EDTA (Y), forms both MHY and MY inner-sphere complexes with Cd(II). The overall kinetic flux for the system is the sum of those for the two types of inner-sphere complexes (Eq. (*7*)). The k_d for CdHY outweighs that for CdY by some six orders of magnitude, which

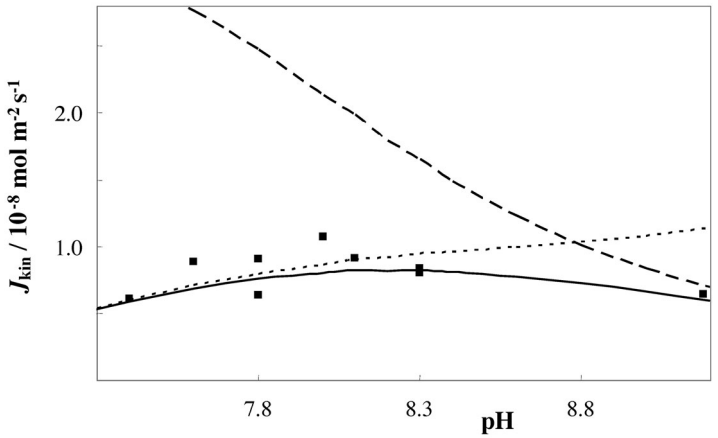

FIG. 2

Comparison of the measured (■) and computed (curves) J_{kin} for Cd(II)–EDDA complexes as a function of pH. The calculated curves are shown for the overall kinetic flux (i) resulting from the outer-sphere precursor complexes $Cd(H_2O)_6L^0$ and $Cd(H_2O)_6HL^+$ (solid curve), (ii) resulting from outer-sphere complex $Cd(H_2O)_6L^0$ only (dashed curve), (iii) resulting from outer-sphere complex $Cd(H_2O)_6HL^+$ only (dotted curve), for a total ligand concentration of 2×10^{-6} mol l^{-1} and a total metal concentration of 4×10^{-7} mol l^{-1}. Parameters used: log $K^{os}(Cd(H_2O)_6L^0)$ = 1.27, log $K^{os}(Cd(H_2O)_6HL^+)$ = 0.36, $k_w = 3 \times 10^8$ s^{-1}, $D_{Cd} = D_{CdL} = 7 \times 10^{-10}$ m^2 s^{-1}, $r_0 = 6 \times 10^{-6}$ m, log K_{CdL} = 8.2. See ref.[12] for experimental details

is reflected in the respective J_{kin} values (Fig. 3). Therefore, the dissociation flux in this system is dominated by CdHY, up to pH ≈ 9, even though it is a minor component of the equilibrium speciation in bulk solution (Fig. 3a).

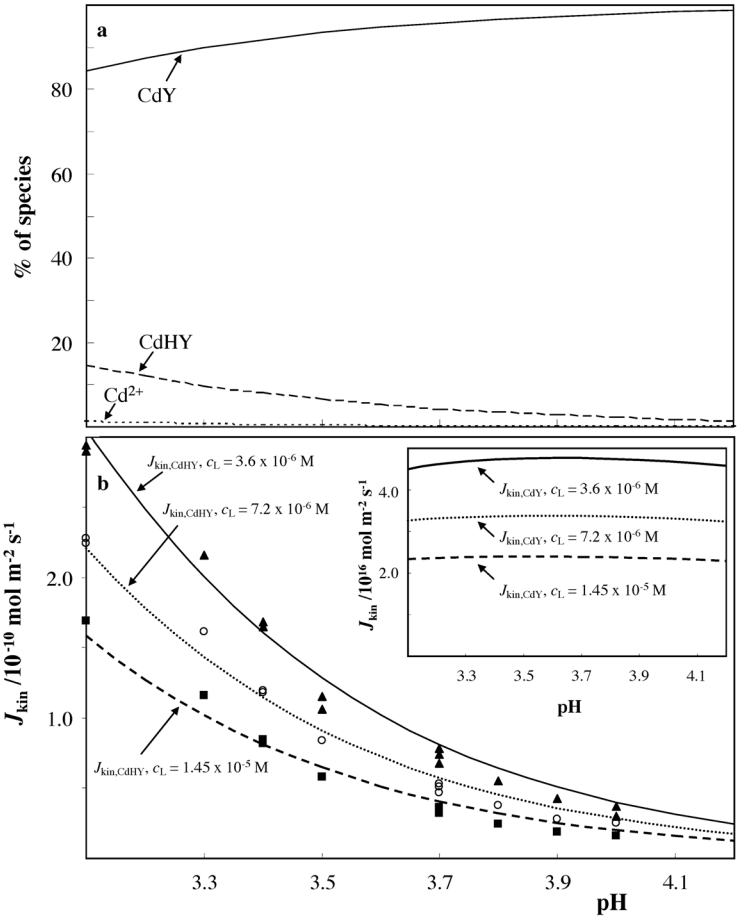

FIG. 3

a Cd(II)–EDTA equilibrium speciation in bulk solution, computed for $c_{Cd,t} = 4 \times 10^{-7}$ and $c_{EDTA,t} = 1.45 \times 10^{-5}$ mol l^{-1}; $K_{CdY} = 10^{16.5}$, $K_{CdHY} = 10^{8.9}$, $K_{1H} = 10^{9.93}$, $K_{2H} = 10^{5.98}$, $K_{3H} = 10^{2.65}$, $K_{4H} = 10^{2.02}$, $K_{5H} = 10^{1.4}$ and $K_{6H} = 10^{0.1}$ l mol^{-1}. b Comparison of the SSCP measured (points) and computed (curves) J_{kin} for CdHY and, in inset, CdY vs pH for Cd(II) complexes with EDTA. Note the scale difference of six orders of magnitude for the inset. The curves are computed for $k_w = 3 \times 10^8$ s^{-1}, $D_{CdL} = D_{CdHL} = 5.3 \times 10^{-10}$ m^2 s^{-1}, $\delta = 1.85 \times 10^{-4}$ m. The results correspond to a total Cd(II) concentration of 4×10^{-7} mol l^{-1} and EDTA concentrations of 3.6×10^{-6} (▲, solid curve), 7.3×10^{-6} (○, dotted curve) and 1.45×10^{-5} mol l^{-1} (■, dashed curve). See ref.[26] for experimental details

In line with this prediction, the J_{kin} values derived from SCP measurements at a conventional electrode are in good agreement with those computed for the CdHY complex as the sole contributor to the dissociation flux (but with the reaction layer thickness defined by all species contributing to the re-association reaction (Eq. (*8*)). The rate of dissociation of CdY, lower by six orders of magnitude, makes its contribution to the overall flux practically negligible under these conditions. This result emphasizes that the impact of protonation on the dissociation of inner-sphere complexes is very different from that at the stage of formation of the outer-sphere complexes.

Higher-Order Inner-Sphere Complexes

For a given ligand L, the stepwise formation constant for 1:1 ML is greater than that for 1:2 ML_2, implying that ML_2 and ML interconvert faster than ML and M. In line with this finding, it has been shown that for systems containing both ML_2 and ML complexes, the step ML → M is the rate-limiting one in the overall process of reduction of metal ions at conventional electrodes and microelectrodes[38,39]. The theoretical framework can be extended to account for the contributions of all various protonated outer-sphere complexes to the rate of complex formation. Ligand protonation appears to be essential in the step ML → M that is relevant for the kinetic flux. The measured microelectrode lability for 1:1 and 1:2 complexes of Cd(II) with pyridine-2,6-dicarboxylic acid (PDCA) is reasonably well described by the differentiated approach, invoking protonation.

Hydroxylated Inner-Sphere Complexes

The importance of hydroxylated inner-sphere complexes for dissociation kinetics is most significant for highly charged ions such as Fe^{3+}, Ti^{3+}, Co^{3+}; divalent ions may also form such complexes, albeit generally at somewhat higher pH, e.g. Cu^{2+} (refs[21,22,40]). For Fe(III), complex species of the types Fe(OH)L and $Fe(OH)_2L$ have been reported for various substituted iminodiacetic acids[41], NTA [42,43], and EDTA[42]. Increased rates of dissociation of Fe(III)–EDTA at higher pH have been ascribed to the kinetic impact of $Fe(OH)_jL$ complexes[44]. Such observations are well explained within the generic framework presented herein. As the Fe(III) ion becomes more hydroxylated, k_w increases dramatically. Hydroxide as a metal complexing agent is of special nature. In contrast to the situation for any other L, conversion of the hydroxide complex $Fe(H_2O)_{6-j}(OH)_j^{3-j}$ to the free metal form,

$Fe(H_2O)_6^{3+}$, only requires protonation of the ligand rather than breaking the Fe^{3+}–O bond. This is very fast and thus it is the equilibrium concentrations of the various protonated/deprotonated species that are relevant for the Fe(III) complex formation/dissociation kinetics. The extent of deprotonation of the hydrated Fe^{3+} ion coordinated in the inner-sphere complex has a substantial impact on k_d since the Fe(III)–OH complex is considerably weaker than its fully protonated congener. Similarly for Co(III), an inner-sphere OH group is reported to accelerate the dissociation of carboxylic acid and chloro complexes[4]. These effects have significant consequences for many biological and technological applications. Thus exploration of the kinetic features of inner-sphere OH complexes merits further attention.

CONCLUSIONS

The influence of (de)protonation of aqueous metal ions and ligands on the chemodynamics of their complexes is shown to be significant for kinetic fluxes measured at conventional electrodes and microelectrodes. The reaction layer formalism, developed for a simple 1:1 ML system, can be generalized to include protonated species. The differentiated analysis shows that the influence of (de)protonated M and L on the rates of formation and dissociation are completely different. The rate of association is defined by the summation over all possible protonated forms of the metal *and* those of the ligand that contribute to μ to an extent weighted by their K^{os} values. Similarly, the dissociation of all the (de)protonated inner-sphere complexes contributes to the overall kinetic flux. The absence or presence of a proton can have a very large impact on k_d (many orders of magnitude), and hence the kinetics can be dominated by a species that is a very minor component of the bulk speciation. In the examples presented here, the overall agreement between the measured and computed J_{kin} is convincing, given the uncertainties in various parameters.

The overall impact of protonation on metal speciation dynamics is that the kinetic flux increases at low pH when a proton displaces M from an inner-sphere binding site on L, MH_iL, and also increases at high pH when a water molecule in the inner hydration sphere of M is deprotonated, giving $M(OH)_jL$. Accordingly, lability passes through a minimum over a pH range determined by the dynamic features of the involved species. For divalent ions, in the acid to circumneutral pH range, MH_iL complexes may dominate the kinetics; for trivalent ions, $M(OH)_jL$ species may be the kinetically most relevant ones at circumneutral pH. An enhanced kinetic flux via a low concentration of a rapidly dissociating complex may be very functional

biologically. For example, microorganisms possess proton pumps which allow biomanipulation of pH in their local environment. This option can be utilized in generating kinetic bypass routes to dissociation into the free metal ion via the acid MHL or the basic $M(OH)_jL$ [45].

SYMBOLS AND ABBREVIATIONS

•	outer-sphere complex
a_g	geometrical center-to-center distance between M and L, m
a_i	center-to-center distance between M and site *i* on L, m
c	concentration, mol l^{-1}
c_M	concentration of all $M(OH)_j$ species, for any *j*, mol l^{-1}
D	diffusion coefficient, m^2 s^{-1}
h_L	maximum number of protonable sites on the ligand L
h_M	maximum number of deprotonable inner-shell water molecules on the metal ion M
i	the number of protons attached to L
j	the number of protons removed from the inner hydration shell of M
J	flux, mol m^{-2} s^{-1}
k_a	complex formation rate constant, l mol^{-1} s^{-1}
k_d	complex dissociation rate constant, s^{-1}
k_w	rate constant for water substitution, s^{-1}
K	stability constant, l mol^{-1}
K^{os}	stability constant for outer-sphere complex, l mol^{-1}
m	charge on fully deprotonated L
N_A	Avogadro constant, mol^{-1}
r_0	radius of microsphere, m
R_a	total rate of complex formation, mol l^{-1} s^{-1}
$\boldsymbol{U}^{os}$	normalized interionic potential for an ion pair, U^{os}/kT, J
δ	diffusion layer thickness, m
κ	reciprocal Debye length, m^{-1}
μ	reaction layer thickness, m
μ_{eff}	effective reaction layer thickness, m
τ_M	lifetime of M, s
ξ	degree of lability, dimensionless
EDDA	1,2-diaminoethane-*N*,*N*′-diacetic acid
EDTA, Y	ethylenediaminetetraacetic acid
KK	Koutecký–Koryta
NTA	nitrilotriacetic acid
PDCA	pyridine-2,6-dicarboxylic acid
SCP	stripping chronopotentiometry
SSCP	stripping chronopotentiometry at scanned deposition potential
SV	stripping voltammetry

REFERENCES

1. van Leeuwen H. P., Town R. M., Buffle J., Cleven R. F. M. J., Davison W., Puy J., van Riemsdijk W. H., Sigg L.: *Environ. Sci. Technol.* **2005**, *39*, 8545.
2. Tanaka N., Tamamushi R., Kodama M.: *Z. Phys. Chem.* **1958**, *14*, 141.
3. Kodama M., Namekawa K., Horiuchi T.: *Bull. Chem. Soc. Jpn.* **1974**, *47*, 2011.
4. Davies G.: *J. Phys. Chem. B* **2007**, *111*, 6955.
5. Koutecký J., Brdička R.: *Collect. Czech. Chem. Commun.* **1947**, *12*, 337.
6. Koryta J.: *Chem. Listy* **1959**, *52*, 2253.
7. Heyrovský J., Kůta J.: *Principles of Polarography*. Academic Press, New York 1966.
8. van Leeuwen H. P., Buffle J.: *Environ. Sci. Technol.* **2009**, *43*, 7175.
9. Eigen M.: *Pure Appl. Chem.* **1963**, *6*, 97.
10. Morel F. M. M., Hering J. G.: *Principles and Applications of Aquatic Chemistry*. Wiley, New York 1993.
11. Eigen M.: *Discuss. Faraday Soc.* **1954**, *17*, 194.
12. van Leeuwen H. P., Town R. M., Buffle J.: *J. Phys. Chem. A* **2007**, *111*, 2115.
13. Dodgen H. W., Liu G., Hunt J. P.: *Inorg. Chem.* **1981**, *20*, 1002.
14. Swaddle R. W., Merbach A. E.: *Inorg. Chem.* **1981**, *20*, 4212.
15. Grant M., Jordan R. B.: *Inorg. Chem.* **1981**, *20*, 55.
16. Schneider W.: *Chimia* **1988**, *42*, 9.
17. Pham A. N., Rose A. L., Freitz A. J., Waite T. D.: *Geochim. Cosmochim. Acta* **2006**, *70*, 640.
18. Davies G., Warnqvist B.: *Coord. Chem. Rev.* **1970**, *5*, 349.
19. Fuoss R.: *J. Am. Chem. Soc.* **1958**, *80*, 5059.
20. Lyklema J.: *Fundamentals of Interface and Colloid Science*, Vol. 1. Academic Press, London 1991.
21. Martell A. E., Chaberek S., Courtney R. C., Westerback S., Hyytiainen H.: *J. Am. Chem. Soc.* **1957**, *79*, 3036.
22. Courtney R. C., Gustafson R. L., Chaberek S., Martell A. E.: *J. Am. Chem. Soc.* **1958**, *80*, 2121.
23. Koutecký J., Koryta J.: *Electrochim. Acta* **1961**, *3*, 318.
24. van Leeuwen H. P., Puy J., Galceran J., Cecília J.: *J. Electroanal. Chem.* **2002**, *526*, 10.
25. Town R. M., van Leeuwen H. P.: *J. Phys. Chem. A* **2008**, *112*, 2563.
26. van Leeuwen H. P., Town R. M.: *Environ. Sci. Technol.* **2009**, *43*, 88.
27. van Leeuwen H. P.: *J. Radioanal. Nucl. Chem.* **2000**, *246*, 487.
28. Buffle J., Startchev K., Galceran J.: *Phys. Chem. Chem. Phys.* **2007**, *9*, 2844.
29. Zhang Z., Buffle J.: *J. Phys. Chem. A* **2009**, *113*, 6562.
30. van Leeuwen H. P.: *J. Electroanal. Chem.* **1979**, *99*, 93.
31. Galceran J., Puy J., Salvador J., Cecília J., van Leeuwen H. P.: *J. Electroanal. Chem.* **2001**, *505*, 85.
32. Town R. M., van Leeuwen H. P.: *Electroanalysis* **2004**, *16*, 458.
33. Town R. M., van Leeuwen H. P.: *J. Electroanal. Chem.* **2002**, *523*, 1.
34. DeFord D. D., Hume D. N.: *J. Am. Chem. Soc.* **1951**, *73*, 5321.
35. van Leeuwen H. P., Town R. M.: *J. Electroanal. Chem.* **2002**, *536*, 129.
36. Town R. M., van Leeuwen H. P.: *J. Electroanal. Chem.* **2003**, *541*, 51.
37. van Leeuwen H. P., Town R. M.: *J. Electroanal. Chem.* **2004**, *561*, 67.
38. Puy J., Cecília J., Galceran J., Town R. M., van Leeuwen H. P.: *J. Electroanal. Chem.* **2004**, *571*, 121.

39. van Leeuwen H. P., Town R. M.: *J. Electroanal. Chem.* **2006**, *587*, 148.
40. Gustafson R. L., Martell A. E.: *J. Am. Chem. Soc.* **1959**, *81*, 525.
41. Sanchiz J., Esparza P., Domínguez S., Brito F., Mederos A.: *Inorg. Chim. Acta* **1999**, *291*, 158.
42. Gustafson R. L., Martell A. E.: *J. Phys. Chem.* **1963**, *67*, 576.
43. Cuculić V., Pižeta I., Branica M.: *Electroanalysis* **2005**, *17*, 2129.
44. Sunda W., Huntsman S.: *Mar. Chem.* **2003**, *84*, 35.
45. Milligan A. J., Mioni C. E., Morel F. M. M.: *Mar. Chem.* **2009**, *114*, 31.